Absence of carrier separation in ambipolar charge and spin drift in p + -GaAs

Fabian Cadiz, D. Paget, A. Rowe, L. Martinelli, S. Arscott

Applied Physics Letters

Absence of carrier separation in ambipolar charge and spin drift in p^+-GaAs

Cite as: Appl. Phys. Lett. **107**, 162101 (2015); https://doi.org/10.1063/1.4933189
Submitted: 03 August 2015 • Accepted: 04 September 2015 • Published Online: 19 October 2015

F. Cadiz, D. Paget, A. C. H. Rowe, et al.

AIP Publishing

Absence of carrier separation in ambipolar charge and spin drift in p^+-GaAs

F. Cadiz,[1] D. Paget,[1] A. C. H. Rowe,[1] L. Martinelli,[1] and S. Arscott[2]
[1]*Physique de la Matière Condensée, Ecole Polytechnique, CNRS, 91128 Palaiseau, France*
[2]*Institut d'Electronique, de Microélectronique et de Nanotechnologie (IEMN), Université de Lille, CNRS, Avenue Poincaré, Cité Scientifique, 59652 Villeneuve d'Ascq, France*

(Received 3 August 2015; accepted 4 September 2015; published online 19 October 2015)

The electric field-induced modifications of the spatial distribution of photoelectrons, photoholes, and electronic spins in optically pumped p^+ GaAs are investigated using a polarized luminescence imaging microscopy. At low pump intensity, application of an electric field reveals the tail of charge and spin density of drifting electrons. These tails disappear when the pump intensity is increased since a slight differential drift of photoelectrons and photoholes causes the buildup of a strong internal electric field. Spatial separation of photoholes and photoelectrons is very weak so that photoholes drift in the same direction as photoelectrons, thus exhibiting a negative effective mobility. In contrast, for a zero electric field, no significant ambipolar diffusive effects are found in the same sample. © *2015 AIP Publishing LLC*. [http://dx.doi.org/10.1063/1.4933189]

Understanding the mechanisms which determine charge and spin currents in bipolar charge and spin devices is crucial for future applications. This understanding requires the investigation of the effects of interactions between electrons and slower drifting holes in an electric field and of their implications for spin transport. Two types of interactions have been considered in the past. First, electron-hole Coulomb drag has been demonstrated in quantum wells and shown to lead to a negative effective mobility of minority electrons,[1–4] an effect which can also be induced more generally by thermal fluctuations,[5] or large concentrations of interacting particles.[6] Second, the differential diffusion and drift of majority and minority carriers lead to the appearance of internal electric fields of ambipolar origin. The effect of this field on charge and spin diffusion, in the absence of an applied electric field, has been investigated in several works.[7–11] On the other hand, effects of electron-hole interactions on charge and spin drift in an electric field have not been widely investigated.[12]

Here, we image charge and spin drift in p^+ GaAs using a polarized microscopy technique described elsewhere.[13] The effect of electron-hole interaction is investigated by generating spin-polarized minority electrons of variable density, using a tightly focused circularly polarized light excitation of variable power (1/e half width of 0.6 μm, energy 1.55 eV). The profile of the luminescence intensity is monitored. This gives the profile integrated over depth of $n = n_+ + n_-$, where $n_\pm$ are the concentrations of electrons of spins $\pm$ along the direction of light excitation. In the same way, monitoring of the spatial profile of $I(\sigma^+) - I(\sigma^-)$, where $I(\sigma^\pm)$ is the intensity of the $\sigma^\pm$-polarized component of the luminescence, gives the depth-integrated profile of $s = n_+ - n_-$.

Sample epitaxial growth was performed starting with a commercial 2 in. diameter semi-insulating (SI) epi-ready GaAs wafer. A GaInP layer was first grown (nominal thickness of 100 nm) confining the photoelectron transport and ensuring that recombination at the back sample interface is negligible. The active GaAs layer has a thickness of 3 μm and is doped p-type using carbon to $N_A = 10^{18}$ cm^{-3}. The surface of this layer is covered with a natural oxide. Hall bars were fabricated [see Fig. 1(a)], using electron beam lithography masking, ohmic contact (platinum-based) metallization and dry etching (chlorine-based) processes.

Panel (b) of Fig. 1 shows the intensity profiles at low power (no ambipolar effects), for a zero applied electric field E and at 15 K. As shown elsewhere,[13] this profile is spatially isotropic, apart from a slight guided signal at the two edges of the structure. Its typical extent reveals the charge diffusion length. Panel (c) of Fig. 1 shows the same profile at $E = 400$ V/cm and shows the drifting of electrons from the formation of an intense tail. This imaging of drift at low power has been investigated before.[14,15] As shown in panels (d) and (e) of Fig. 1, an increase of excitation power progressively removes the tail of drifting electrons, which seems to be almost completely absent in panel (e). These results will be attributed to ambipolar coupling between electrons and holes since the internal field of ambipolar origin opposes to outward drift and tends to drive the photoelectrons back to the excitation spot. This internal field essentially lies parallel to the surface and is of the same origin as the Dember field which rather characterizes ambipolar transport perpendicular to the surface.[16]

These results are shown in more detail in Fig. 2, which presents the section of these profiles along the direction of the electric field and the signal at $r = 0$ normalized to the excitation power. Panel (b) shows that, when the excitation power is increased, an important charge accumulation occurs at the place of excitation, giving rise to an increase of the normalized signal at $r = 0$. On the other hand, the slope of the profile at large distance is determined by the local charge concentrations and is weakly dependent on excitation power. A similar effect is exhibited by the spin density, as shown in panel (a) of Fig. 3.

In contrast, as shown in panel (a) of Fig. 2, if no electric field is applied, the section weakly depends on power, and the normalized signal at $r = 0$ is constant. This shows that, for $N_A = 10^{18}$ cm^{-3}, ambipolar diffusion effects are relatively weak for the present range of excitation powers. The fact that ambipolar effects affect more the drift than the

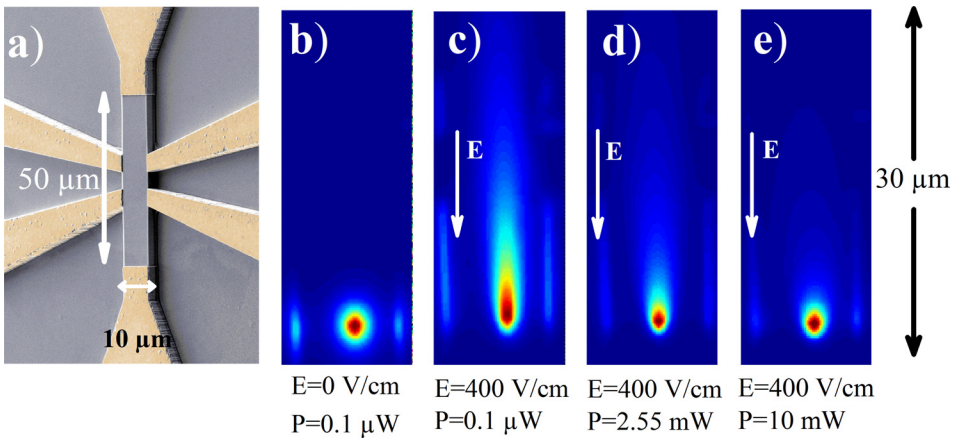

FIG. 1. Panel (a) shows an SEM image of the p-GaAs hall bar used to study ambipolar charge and spin drift. Panels (b)–(e) show the intensity profiles for selected values of electric field and power. The photoelectron tail, seen to appear in panel (c) because of drift in the electric field, is progressively reduced when the excitation power is increased, as a consequence of the internal electric field caused by slower drifting photoholes (ambipolar drift).

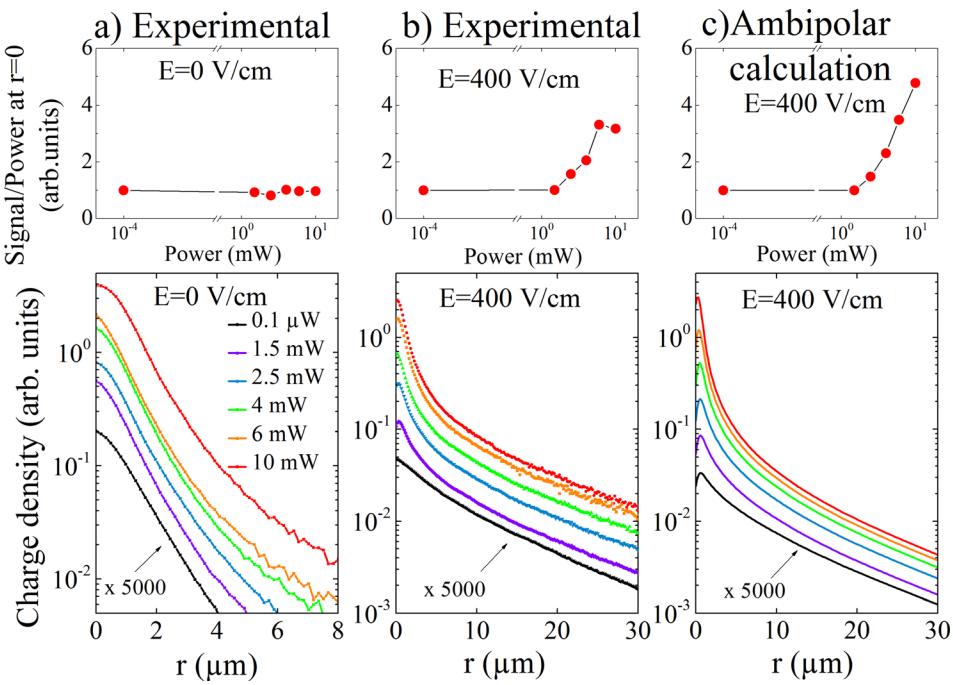

FIG. 2. Each panel shows in the lower part the intensity profile along the direction of the Hall bar for several excitation powers, while the upper part shows the corresponding signal at $r = 0$, normalized to the excitation power. Panel (a) illustrates the case of a zero electric field. The weak dependence of the shapes of these profiles as a function of excitation power, and the power independence of the normalized signal at $r = 0$ reveal the relative weakness of ambipolar diffusion effects for the present sample. Panel (b) shows the same results for $E = 400$ V/cm, revealing the importance of ambipolar drift from the relative increase of the signal at $r = 0$. Panel (c) shows the profiles and normalized signal at $r = 0$ calculated using Eq. (4) and assuming local charge neutrality.

diffusion of photocarriers is directly related to the large difference between the unipolar displacements of photoelectron and photohole clouds. For diffusive transport ($E = 0$), the overall relative displacement is zero, so that only the extensions of the electron and hole clouds differ. Conversely, for drift transport, the clouds are, in a unipolar model, separated by the sum of electron and hole drift lengths $(\mu_e + \mu_h)\tau E$, where μ_e and μ_h are the electron and hole mobilities, respectively, and τ is the lifetime. This generates a significantly stronger internal electric field.

For interpreting the results of Figs. 1–3, effects of the Pauli Principle on the charge and spin diffusivities, as well as possible thermoelectric effects in the spatial gradient of the electronic temperature,[17] will be neglected here, since their effect on ambipolar diffusion is weak. In the same way, it is assumed that Coulomb drag between minority electrons and holes is negligible.[1,3] This effect should also manifest itself at low excitation power when an electric field is applied, thus increasing the velocity of majority holes. Since in this case the peak of the spatial photoelectron distribution is not observed to shift, this effect can be excluded (see Fig. 3 of Ref. 15). The fact that Coulomb drag effects are negligible has been attributed to the small hole mobility in bulk GaAs, with respect to modulation-doped quantum wells[2] and, in the present strongly doped sample, to screening of the electrostatic interactions by the hole gas.[17]

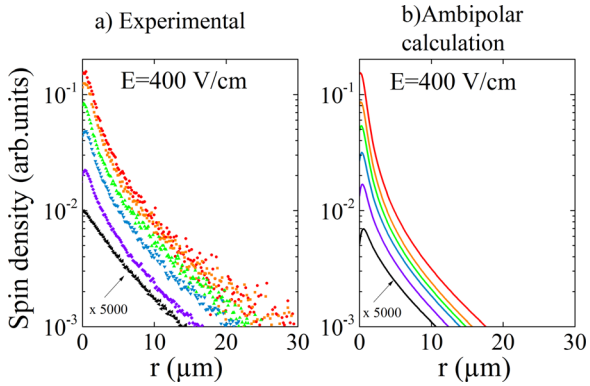

FIG. 3. Panel (a) shows the spatial profile of $s = n_+ - n_-$ for increasing values of excitation power, and in the same conditions as panel (b) of Fig. 2(a). This reveals that spin density is also sensitive to ambipolar drift. Panel (b) shows the results of calculations using Eq. (8) assuming that photoelectrons and photoholes are not separated by the applied field.

In this framework, modeling of ambipolar drift is performed by calculating first the total electric field $\vec{E}_{tot}$. The electron and hole charge conservation equations can be written

$$(g_+ + g_-) - n/\tau + \vec{\nabla} \cdot \vec{J}_e/q = 0, \quad (1)$$

$$(g_+ + g_-) - n/\tau - \vec{\nabla} \cdot \vec{J}_h/q = 0. \quad (2)$$

Here, q is the absolute value of the electronic charge, and $g_\pm$ are the creation rates of electrons of $\pm$ spin. Here, assuming that electron-hole radiative recombination is dominant over other recombination processes, one has $1/\tau = K(N_A + \delta p)$, where K is the bimolecular recombination coefficient and δp is the photohole concentration. As usual, the electron and hole currents are the sum of drift and diffusive currents, and are given by $\vec{J}_e = \sigma_e \vec{E}_{tot} + qD_e \vec{\nabla} n$ and $\vec{J}_h = \sigma_h \vec{E}_{tot} - qD_h \vec{\nabla} \delta p$. The quantity D_h is the hole diffusivity and D_e is the electron charge diffusivity. The conductivities are given by $\sigma_e = q\mu_e n$ and $\sigma_h = q\mu_h(N_A^- + \delta p)$, where N_A^- is the concentration of charged acceptors. Equating Eqs. (1) and (2) and neglecting diffusive transport perpendicular to the surface, one finds

$$\frac{(\sigma_e + \sigma_h)}{q} \vec{E}_{tot} = (D_h - D_e)\vec{\nabla} n + \mu_h N_A^- \vec{E} + D_h \vec{\nabla}(\delta p - n), \quad (3)$$

where the first term is the internal field caused by the distinct diffusions of electrons and holes and aims at restoring the charge neutrality. The second term differs from the applied electric field because of ambipolar drift. The third term accounts for possible departure from local charge neutrality and will be shown below to be negligible in steady-state. Using Eq. (3), the electron and hole currents can be written

$$\vec{J}_e/q = \mu_a n \vec{E} + D_a \vec{\nabla} n + \frac{D_h \sigma_e}{(\sigma_e + \sigma_h)} \vec{\nabla}(\delta p - n), \quad (4)$$

$$\vec{J}_h/q = \frac{\mu_a \mu_h}{\mu_e}(N_A^- + \delta p)\vec{E} - D_a \vec{\nabla} \delta p - \frac{D_e \sigma_h}{(\sigma_e + \sigma_h)} \vec{\nabla}(\delta p - n), \quad (5)$$

where the ambipolar diffusivity and mobility are given by

$$D_a = \frac{\sigma_e D_h + \sigma_h D_e}{\sigma_e + \sigma_h}, \quad (6)$$

$$\mu_a = \mu_e \frac{q\mu_h N_A^-}{\sigma_e + \sigma_h}. \quad (7)$$

Note that the latter expression for μ_a differs from that of Ref. 7, since the electric field which appears in Eq. (4) is the applied field rather than the total field.

The final expressions of the conservation equations are readily obtained by replacing in Eqs. (1) and (2) the electron and hole currents by their values given by Eqs. (4) and (5). Using the same approach, one finds the following expression for the spin conservation equation:

$$(g_+ - g_-) - s/\tau_s + \vec{\nabla} \cdot [\mu_a s \vec{E} + D_a \vec{\nabla} s + D'_a n \vec{\nabla} \mathscr{P} + D''_a \vec{\nabla}(\delta p - n)] = 0, \quad (8)$$

where $1/\tau_s = 1/\tau + 1/T_1$ and T_1 is the spin relaxation time, $(\sigma_e + \sigma_h)D'_a = \sigma_e(D_e - D_h)$ and $(\sigma_e + \sigma_h)D''_a = D_h q s \mu_n$. Here, the spin diffusivity has been taken equal to the charge one, since spin Coulomb drag effects are negligible at this doping because of screening by holes.[17] In order to solve Eqs. (1), (2), and (8), one uses boundary conditions at the top and the bottom film surfaces assuming negligible surface recombination.[18,19] It is first be assumed that majority and minority photocarriers are not separated by the electric field, so that $\delta p = n$. Second, the term $D'_a n \vec{\nabla} \mathscr{P}$ in Eq. (8) is neglected. The latter assumption is legitimate if the polarization is spatially constant and also in the present case since, as found in panel (a) of Fig. 2, diffusion is negligible with respect to drift. As a result of the latter approximations, unlike the case of ambipolar diffusion for which the term $D'_a n \vec{\nabla} \mathscr{P}$ induces a spin-spin coupling at lower doping level,[20] ambipolar drift does not cause an additional coupling mechanism. Thus, the spin density drifts like charge, as characterized by the same ambipolar mobility μ_a and diffusivity D_a.

The values of all the relevant parameters have been determined previously using time-resolved[19] and transport[15] measurements. These values at 15 K and for an electronic temperature $T_e = 53$ K are $\mu_e = 11000$ cm^2/V s, $\mu_h = 100$ cm^2/V s, $D_e = 47$ cm^2/s, $D_h = 0.47$ cm^2/s, $\tau = 360$ ps, and $T_1 = 1050$ ps. Using these values, the normalized charge profiles, calculated using Eqs. (1) and (4), are shown in panel (c) of Fig. 2 and are in satisfactory agreement with the experimental results. The slight difference observed at the maximum excitation power, for which the calculated signal is larger than the experimental one, is attributed to heating of the electron gas. The spin density profiles, calculated using Eq. (8), are shown in panel (b) of Fig. 3 and are also in satisfactory agreement with the experimental results.

The good correspondence between the experimental results and the simplified calculation suggests that the approximation of local neutrality is valid. This approximation is now discussed in more detail by calculating rather the spatial distributions of electron and hole charges using a numerical resolution of Eqs. (1) and (2), using Eqs. (4), (5), and Poisson's equation $\vec{\nabla} \cdot \vec{E}_{tot} = (q/\epsilon\epsilon_0)(\delta p - n)$, where ϵ_0 is the permittivity of vacuum and ϵ is the dielectric constant. A key result is that the internal electric field of ambipolar origin almost totally prevents the separation of photoexcited carriers, so that $n = \delta p$. As shown in panel (b) of Fig. 4, the relative photoinduced electric charge $|(n - \delta p)/(n + \delta p)|$ is always smaller than 10^{-2} so that the assumption of local charge neutrality is fully justified. The departure from neutrality, implying a slight downfield increase of hole concentration and a weaker upfield increase of electron concentration, is sufficient to generate a significant internal electric field of ambipolar origin enabling to reach a self-consistent equilibrium. The calculated spatial dependence of the electric field, for $E = 400$ V/cm, is shown in panel (c) of Fig. 4 as a function of excitation power. This field is comparable with E at all powers apart from the smallest one of 0.1μW and is even larger than E near $r = 0.5\mu$ for the highest power.

The displacement of photoholes adjusts in a self-consistent way under the effect of the internal field, which is

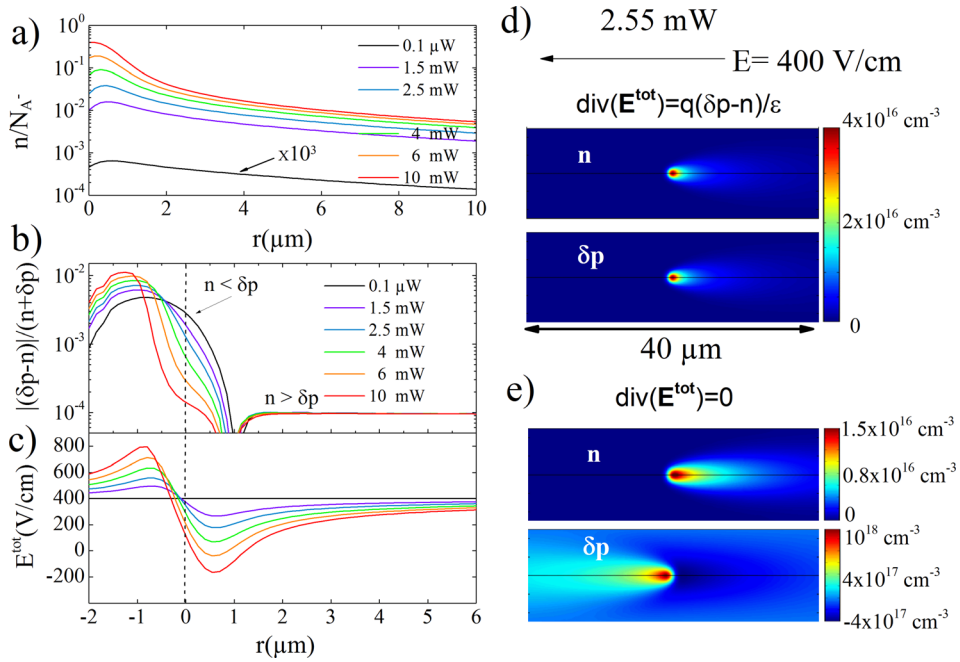

FIG. 4. Panel (a) shows the calculated spatial dependence of the relative photoelectron density n/N_A for an applied field of 400 V/cm and for increasing values of the excitation power. Panel (b) shows in the same conditions, the relative difference between the photoelectron and photohole density, thus revealing quasi-neutrality, and Panel (c) shows the total electric field, defined as the sum of the externally applied field $\vec{E}$ and of the internal field of ambipolar origin. In spite of the weak relative difference between the local electron and hole charges, the latter field can be larger than E at high power and near the place of excitation. Panel (d) shows the identical spatial distributions of photoelectrons and photoholes, as implied by charge neutrality. Panel (e) shows the two corresponding spatial charge distributions in a unipolar regime (replacing the Poisson equation by $\vec{\nabla} \cdot \vec{E} = 0$). These distributions are in opposite directions, which shows that the neutrality is a direct consequence of the Poisson equation.

responsible for the third term in Eq. (5) and depends on the photocarrier distributions. Local charge quasi-neutrality implies that, in steady-state, this displacement follows the drift displacement of electrons and therefore is opposite to the direction of the hole drift current (negative effective hole mobility). This effect is illustrated in more detail in panel (d) of Fig. 4, which shows that the calculated spatial distributions of photoelectrons and photoholes at an excitation power of 2.55 mW are identical. In contrast, if one neglects the electrostatic interaction between electrons and holes, by replacing Poisson's equation by $\vec{\nabla} \cdot \vec{E} = 0$, the hole spatial distribution recovers its unipolar drifting direction, opposite to that of electrons (see panel (e) of Fig. 4).

The calculations show that the minority and majority photocarriers are not separated, (i) even for the smallest excitation power at which, as shown in panel (c), the total field is very close to the applied field, implying that a very small internal electric field is sufficient to restore quasi-neutrality, (ii) up to electric fields as high as 1 kV/cm at which heating of the carriers becomes significant. This result can be interpreted by estimating the order of magnitude of the internal electric field that the electron-hole system can generate in a unipolar regime, assuming maximum separation of electrons and holes. Taking, as shown in panel (a) of Fig. 4, a maximum electronic concentration at high power slightly smaller than N_A, assuming that this concentration extends over a typical volume of 1 μm^3 and that in a unipolar regime holes and electrons are separated by the sum of electron and hole drift lengths, we calculate a very large maximum internal field, of the order of several 10^6 V/cm. This implies that even a very slight departure from local neutrality will generate large internal fields, and will have very strong feedback effects on carrier distribution, thus imposing quasi-neutrality.

In conclusion, the present work has three main results. First, ambipolar electrostatic couplings strongly affect drift transport, but for a zero applied electric field only weakly modifies the concentration profile and therefore the diffusivity. Second, unlike for ambipolar diffusion, the spin density drifts in the same way as charge so that ambipolar drift should modify the behavior of future bipolar spin transistors. Third, the effect of the internal electric field is to restore a quasi-neutrality in the whole space near the excitation spot. This field is comparable, and even larger at high excitation power than the applied electric field. Quasi neutrality implies that majority and minority photocarriers are not separated, so that photohole drift is determined by photoelectron drift and not by the electric field direction. As a result, ambipolar coupling provides a mechanism for effective negative mobility of majority carriers, along with the other processes considered in the introduction.[1–3,5,6]

[1]R. A. Hopfel, J. Shah, P. A. Wolff, and A. Gossard, Phys. Rev. Lett. **56**, 2736 (1986).
[2]R. A. Hopfel, J. Shah, P. A. Wolff, and A. Gossard, Phys. Rev. B **37**, 6941 (1988).
[3]K. Shen and G. Vignale, Phys. Rev. Lett. **110**, 096601 (2013).
[4]G. Vignale, Physics **4**, 48 (2011).
[5]L. Machura, M. Kostur, P. Talkner, J. Luczka, and P. Hanggi, Phys. Rev. Lett. **98**, 040601 (2007).
[6]G. Benichou, P. Ilien, G. Oshanin, A. Sarracino, and R. Voituriez, Phys. Rev. Lett. **113**, 268002 (2014).

[7]R. A. Smith, *Semiconductors* (Cambridge University Press, Cambridge, 1978).
[8]H. Zhao, M. Mower, and G. Vignale, Phys. Rev. B **79**, 115321 (2009).
[9]D. Paget, F. Cadiz, A. C. H. Rowe, F. Moreau, S. Arscott, and E. Peytavit, J. Appl. Phys. **111**, 123720 (2012).
[10]K. Ikeda and H. Kawaguchi, J. Appl. Phys **117**, 053903 (2015).
[11]B. A. Ruzicka, L. K. Werake, H. Samessekou, and H. Zhao, Appl. Phys. Lett. **97**, 262119 (2010).
[12]M. Beck, D. Streb, M. Vitzethum, P. Kiesel, S. Malzer, C. Metzner, and G. H. Dohler, Phys. Rev. B **64**, 085307 (2001).
[13]I. Favorskiy, D. Vu, E. Peytavit, S. Arscott, D. Paget, and A. C. H. Rowe, Rev. Sci. Instrum. **81**, 103902 (2010).
[14]D. Luber, F. Bradley, N. Haegel, M. Talmadge, M. Coleman, and T. Boone, Appl. Phys. Lett. **88**, 163509 (2006).
[15]F. Cadiz, D. Paget, A. C. H. Rowe, E. Peytavit, and S. Arscott, Appl. Phys. Lett. **106**(9), 092108 (2015).
[16]M. Krcemar and W. M. Saslow, Phys. Rev. B **65**, 233313 (2002).
[17]F. Cadiz, D. Paget, A. C. H. Rowe, T. Amand, P. Barate, and S. Arscott, Phys. Rev. B **91**, 165203 (2015).
[18]This approximation is valid for the back surface, because of the presence of the passivating GaInP layer. For the top, naturally oxidized surface, the weak effect of surface recombination in our low temperature regime results, as shown in Ref. 19, in a slight modification of the effective lifetime.
[19]F. Cadiz, P. Barate, D. Paget, D. Grebenkov, J. P. Korb, A. C. H. Rowe, T. Amand, S. Arscott, and E. Peytavit, J. Appl. Phys. **116**, 023711 (2014).
[20]F. Cadiz, D. Paget, A. C. H. Rowe, and S. Arscott, Phys. Rev B **92**, 121203(R) (2015).